Pharmaceutical Research, Vol. 26, No. 12, December 2009 (© 2009)
DOI: 10.1007/s11095-009-9973-4

Research Paper

Preparation, Characterization and Evaluation of Targeting Potential of Amphotericin B-Loaded Engineered PLGA Nanoparticles

Manoj Nahar[1] and Narendra K. Jain[1,2]

Received May 9, 2009; accepted September 14, 2009; published online October 20, 2009

Purpose. The objective of present work was to develop a mannose-anchored, engineered nanoparticulate system for efficient delivery of amphotericin B to macrophages. Furthermore, the effect of spacer on macrophage targeting was also evaluated.
Methods. PLGA was conjugated to mannose via direct coupling (M-PLGA) and via PEG spacer (M-PEG-PLGA), and engineered PLGA nanoparticles (M-PNPs and M-PEG-PNPs) were prepared from respective conjugates. These prepared engineered PNPs were characterized for size, polydispersity index (PDI), surface charge, and drug entrapment efficiency (% DEE). Transmission electron microscopy (TEM) and atomic force microscopy (AFM) were employed to study the shape and surface morphology of engineered PNPs. Macrophage targeting was evaluated via cellular uptake, *ex vivo* antileishmanial activity and *in vivo* biodisposition pattern of engineered PNPs in macrophage-rich organs.
Results. The developed engineered PNPs were found to be of nanometric size (<200 nm) and to have low PDI (<0.162) and good entrapment efficiency (%DEE >53.0%). AFM and TEM revealed that both M-PNPs and M-PEG-PNPs had smooth surface and spherical topography. Engineered PNPs with spacer showed enhanced uptake, potential antileishmanial activity and higher disposition in macrophage-rich organs, suggesting improved macrophage targeting.
Conclusions. The results suggest that engineering of nanoparticles could lead to development of efficient carrier for macrophage targeting.

KEY WORDS: Amphotericin B; J774A.1 Cell; macrophages; nanoparticles; spacer.

INTRODUCTION

Nanoparticulate drug delivery represents a viable option in current chemotherapy. Nanoparticulate carriers have always been attractive due to their size and ability of spatial and temporal controlled delivery of bioactives (1). Particulate drug carriers can substantially influence not only pharmacokinetics but also biodistribution of the drug (2). The ability of particulate carriers to be taken up by mononuclear phagocyte system (MPS) makes them an ideal vehicle for selective transport of drug to target tissues in disease where phagocytic cells are involved. The particulate nature of these vehicles may facilitate passive homing of the entrapped drug molecules to the macrophages, which may harbor many of the important pathogens in their intracellular compartments, such as mycobacterium, leishmania and dengue virus, etc. (3). However, most of these nano-carriers failed to deliver the drug to diseased area efficiently due to non-specific MPS uptake and poor target specificity. The natural passive uptake suffers from many inherent drawbacks, like poor drainage at the site of injection and non-homogeneous distribution to various macrophage specific tissues. Further, active targeting also suffers from some inherent problems like desorption and lack of orientation of ligand for efficient receptor-mediated endocytosis (RME). However, appropriate modifications and engineering of the surfaces of these carriers may result in more efficient targeting of the bioactives to specific targets. Surface modification of these carriers with site-specific ligands further facilitates their rate and extent of uptake by RME (4).

Out of a large array of particulate carrier, polymeric nanoparticles are well-established for drug delivery, specifically PLGA-based nanoparticles (PNPs) due to their well-known inherent advantages. Polymeric nanoparticles can be actively targeted via easier ligation with site-specific ligands that in turn enhance target specificity and performance efficiency. Site-specific ligands can be anchored either by covalent or physical adsorption to the carrier. However, adsorption or coating of ligands is undesirable owing to rapid desorption of ligand coating when they interact with blood components. Further, direct coupling of ligand to carrier (without spacer) may cause decreased propensity of interaction with receptor due to improper orientation of ligand (5). Therefore, we hypothesized the use of ligand-anchored carrier with spacer like PEG that could alter the targeting

[1] Pharmaceutics Research Laboratory, Department of Pharmaceutical Sciences, Dr. Hari Singh Gour University, Sagar 470003, India.
[2] To whom correspondence should be addressed. (e-mail: jnarendr@yahoo.co.in)

potential of carrier in macrophages. Spacer provides flexibility, accessibility and minimal steric hindrance to ligands to interact with receptor efficiently. Earlier reports of PLGA coupling with lectin mostly employed post-conjugation methods (6,7). These methods may degrade or release entrapped drug due to harsh chemical milieu and longer duration of chemical reactions. Therefore, we proposed preparation of engineered NPs using ligand-polymer conjugate, which could serve as platform technique in designing engineered NPs for site-specific delivery (8). Further, size of NPs was maintained between 150–250 nm in order to aid the uptake and tissue distribution to all macrophage rich tissues.

The exclusive presence of mannose receptors on macrophages has been exploited for developing an efficient macrophage-directed drug carrier (2,9–11). Mukhopadhya and Basu (12) reviewed the intracellular delivery of drugs to macrophages by RME using mannose and scavenger receptors for various macrophage-specific diseases like visceral leishmaniasis (VL). Previously, cytotoxic drugs, such as methotrexate and doxorubicin, were conjugated to mannose-specific neoglycoproteins for active targeting to macrophages and were found to be highly effective against VL (11,13). Several groups have generated mannose-coated liposomes for selective delivery of drug to macrophages exploiting the phagocytic properties of the mannose receptor. Approaches for targeting liposomes to macrophages include mannosylation of preformed liposomes (14,15), formation of liposomes from mannosylated phospholipids (16) or grafting a mannose terminal protein on the liposome surface (17). Kassab *et al.* (7) previously developed biodegradable amphotericin B (AmB)-loaded galactosylated poly (l-lactic acid) (l-PLA) and poly (l-lactic-co-glycolic acid) (PLGA) microspheres. The developed system was specifically recognized by *K. bulgaricus* yeasts, which bear galactose specific lectin. Moreover, macrophages upon interaction with particulate drug delivery vehicles may act as secondary drug depot, thus helping in localized delivery of the drug at the infected sites (3,4).

Therefore, proposed methodology encompasses inclusion of the macrophage's receptor-specific ligand (mannose) on nanoparticulate surface, which may significantly enhance the rate and extent of uptake and provide controlled delivery of bio-actives for treatment of macrophages-specific diseases like VL, human immunodeficiency virus (HIV), tuberculosis, etc. Inclusion of spacer could further enhance the target specificity and performance efficiency.

MATERIALS AND METHODS

Materials

Poly (DL-lactic/glycolic acid) (PLGA) 50:50 (RG 502H) with inherent viscosity 0.16–0.24 dl/g, acid number (>6 mg KOH/g), and molecular weight (13,500 Da) was procured from Boehringer Ingelheim (Ingelheim, Germany). Acetone, ethanol, dimethyl sulfoxide (DMSO) and acetonitrile were purchased from Central Drug House (New Delhi, India). Sodium cholate (99%) was procured from Otto (Mumbai, India). N-hydroxysulfosuccinimide (NHS) and dicyclocarbodiimide (DCC) were procured from Rankem (Mumbai, India). (4-(2-Hydroxyethyl)-1-piperazineethanesulfonic acid)(HEPES) buffer, PEG diamine 3400 D ($PEG_{3.4KD}$ diamine), rhodamine isothiocynate (RITC), amberlite XAD 16 resin were purchased from Sigma Chemical Co. (St Louis, MO, USA). Amphotericin B was a generous gift by M/s Dabur India Ltd. (Ghaziabad, UP, India). All others chemicals were of analytical reagent grade and used as received. Triple distilled deionized water was used for all experiments.

Synthesis and Characterization of Mannose-PLGA Conjugates With or without Spacer

The mannose-PLGA conjugate without spacer (M-PLGA) was synthesized by reported method with slight modifications (18). Briefly, calculated quantity of PLGA (0.037 mmol) was dissolved in 10 mL dichloromethane (DCM), and DCC and NHS were added in five molar excess in order to activate free carboxylic group of PLGA. The precipitated dicylco hexyl urea was removed by filtration, while the excess of NHS and DCC were removed by dialysis against distilled water for 6 h. Ethylenediamine (EDA; 160 μL, 0.003 μmol) was added to the above solution, pH of the mixture was adjusted to about 5.0 by addition of 1 N HCl. This resulted in amine-terminated PLGA. The mannose was conjugated to amine-terminated PLGA using reported method with slight modifications (19). Briefly, amine-terminated PLGA (0.1 mmol) was dissolved in 2 mL tetrahydrofuran, D-mannose (8 mM) in 0.1 M sodium acetate buffer (pH 4.0) was added, and the mixture was agitated at ambient temperature for 2 days to ensure completion of reaction. The final solution was transferred to dialysis bag (12 kDa, MWCO, Himedia, Mumbai, India) and dialyzed against distilled water for 24 h. The scheme of synthesis is presented in Fig. 1A. The structure of M-PLGA was confirmed by FTIR (Fig. 2A). For the synthesis of RITC-anchored PLGA, RITC (250 μL, 1 mg/mL) solution in dimethyl formamide was added to the amine-terminated PLGA (5 mg, 0.37 μmol) and stirred at 600 rpm for 1 h at 40 ± 1°C.

Mannose-conjugated PLGA via PEG spacer (M-PEG-PLGA) was synthesized using t-BOC-protected $PEG_{3.4KD}$ diamine as spacer. Mannose was conjugated to t-BOC-protected $PEG_{3.4KD}$ diamine using reported method (19). Mannose t-BOC-protected $PEG_{3.4KD}$ was further conjugated to PLGA using carbodiimide reaction, after t-BOC deprotection (using 0.1 N $KHSO_4$). Briefly, calculated quantity of PLGA (0.037 mmol) was dissolved in 10 mL DCM in order to activate free carboxylic group of PLGA. Thereafter, five molar excess of DCC and NHS were added. The DCU precipitate formed was removed by filtration. The excess of NHS and DCC were removed by dialysis against distilled water. The mannose-$PEG_{3.4K}$ (50 mg, 0.0138 mmol) was added to NHS activated PLGA, resulting into mannose-PEG-PLGA (M-PEG-PLGA). The scheme of synthesis is presented in Fig. 1B. The structure of M-PEG-PLGA was confirmed by FTIR (Fig. 2B)

Preparation of Engineered PNPs

Plain PLGA nanoparticles (PNPs), mannose-anchored PNPs without spacer (M-PNPs) and mannose-anchored PNPs with PEG spacer (M-PEG-PNPs) were prepared by an emulsion solvent evaporation (o/w emulsification) technique (20). Initially, specified amount of PLGA (50 mg) was

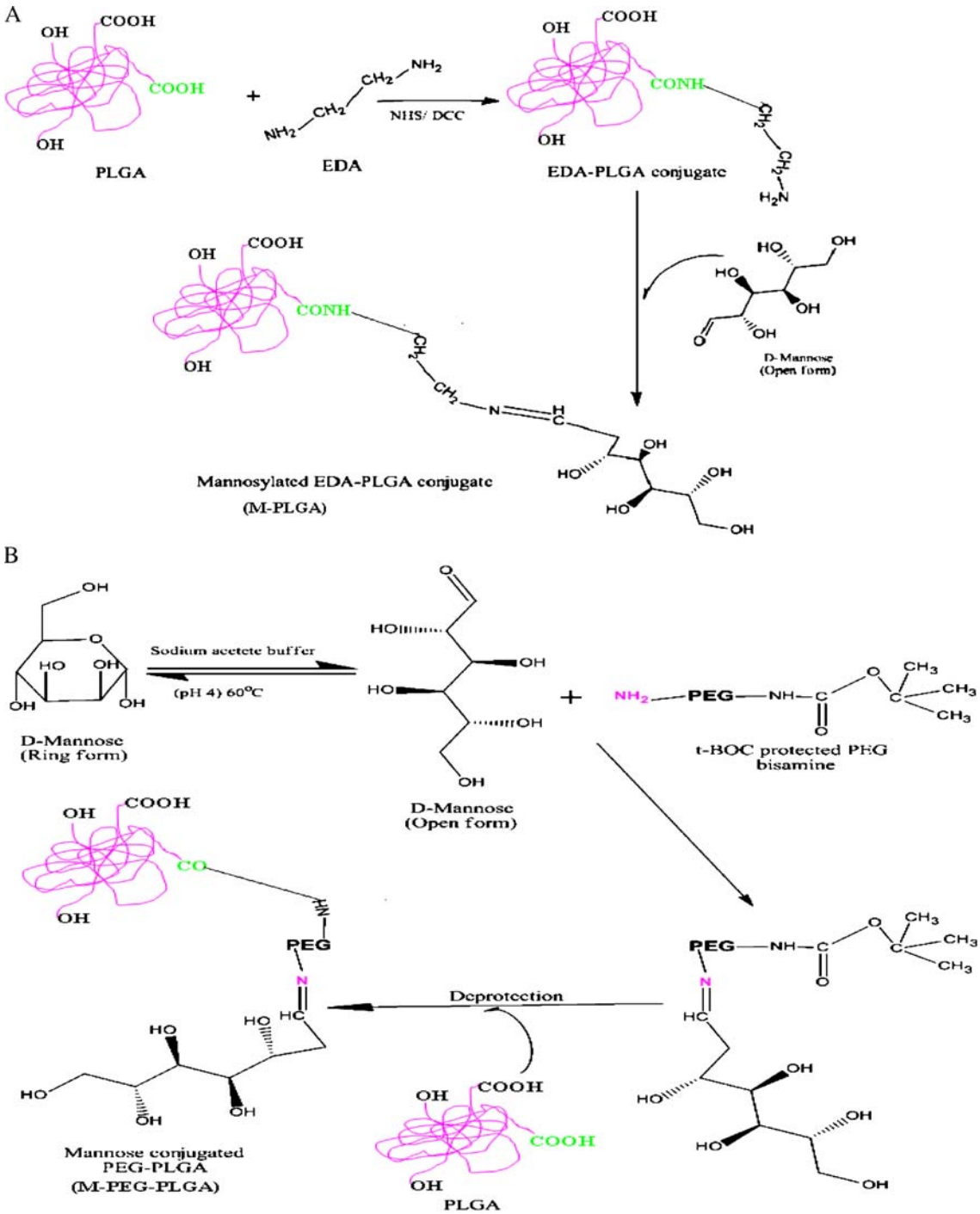

Fig. 1. Scheme of synthesis of mannose-PLGA conjugates; (**A**) without spacer (M-PLGA), (**B**) with PEG spacer (M-PEG-PLGA).

dissolved with or without drug in 2 mL mixture of DMSO: DCM (30:70% v/v), acidified to pH 3.0 with acetic acid, vortexed and emulsified with 20 mL sodium cholate solution (0.02 % w/v) in a sonicator (Sonics-Vibra Cell, BC-130, Ultra sonic processor, CT, USA) at 40 W output for 60 seconds. The organic solvent was evaporated at room temperature for 6 h. PNPs were then recovered by centrifugation (44,250Xg, 20 min, 4°C; Z 36 HK, Hermle Labortechnik GmbH Wehingen, Germany). M-PNPs and M-PEG-PNPs were prepared using mixture of M-PLGA and M-PEG-PLGA conjugate with PLGA (50% w/w). Similarly, RITC-labeled PNPs were prepared by replacing 500μg RITC-PLGA conjugate with PLGA. The rest of the procedure was similar to that followed for the preparation of PNPs. The PNPs were then washed twice with water, and unentrapped drug was removed using amberlite resin XAD 16 (20) and finally lyophilized. The dried PNPs were stored in the refrigerator at 4°C.

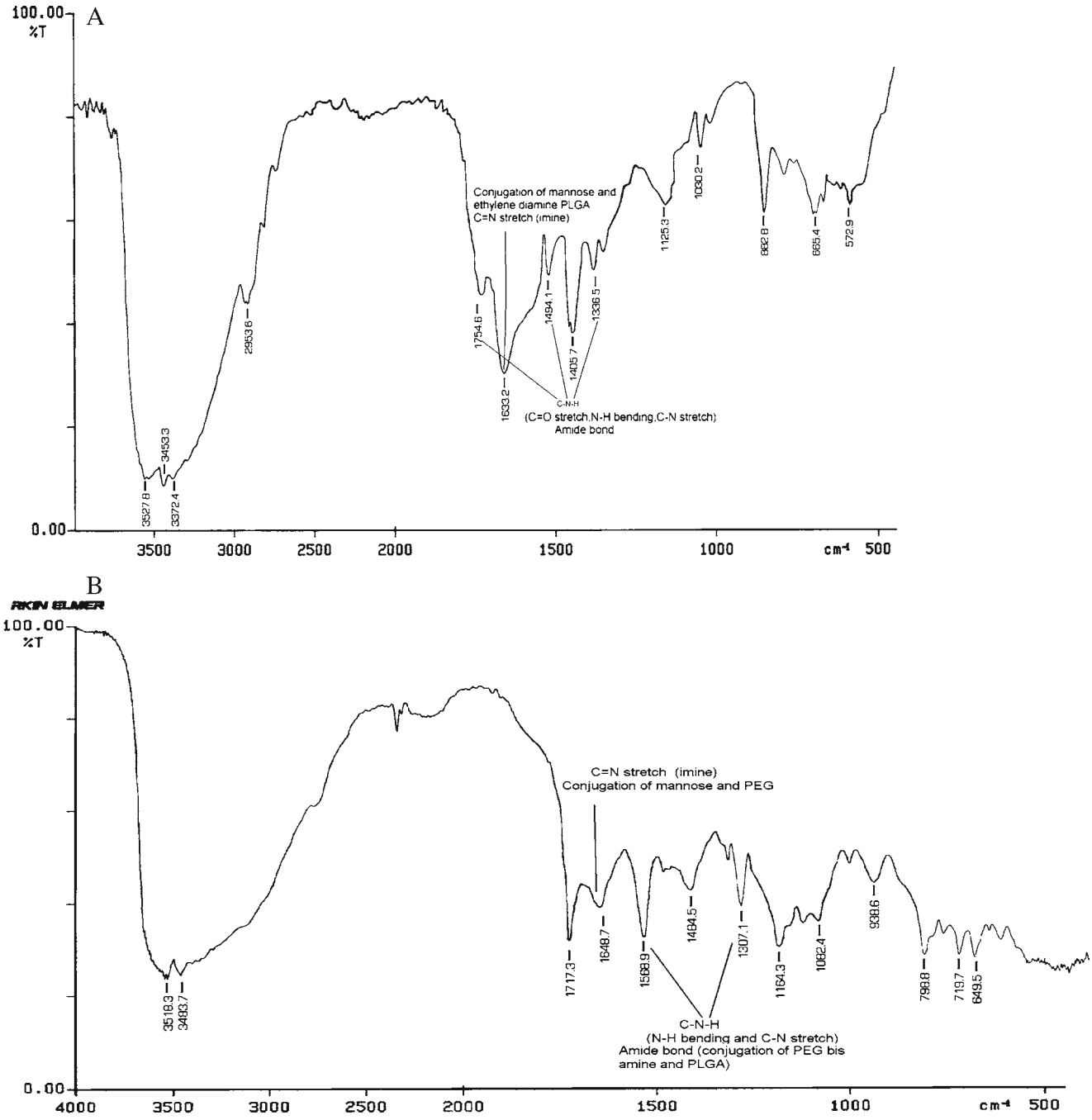

Fig. 2. FTIR spectrum of mannose-PLGA conjugates; (**A**) without spacer (M-PLGA), (**B**) with PEG spacer (M-PEG-PLGA).

Particle Size, Surface Charge and Polydispersity Index (PDI)

The particle size, PDI and surface charge were determined in a Malvern Zetasizer (NanoZS, Malvern Instruments Inc., Worcestershire, UK). Particle size and PDI of M-PNPs and M-PEG-PNPs were determined by light scattering method based on laser diffraction at angle 135^0. Typically, engineered PNPs were suspended in aqueous medium (1.5 mL) and placed in a couvette at a concentration of 0.3 mg/mL at 25±1°C. The viscosity and refractive index of the continuous phase were set to those specific to water. Engineered PNPs, surface charge was determined by laser doppler anemometry using Malvern Zetasizer (NanoZS, Malvern Instruments Inc., Worcestershire, UK). Engineered PNPs were suspended in 1 mM HEPES buffer and adjusted to pH 7.4 by 0.1 M HCl in order to maintain a constant ionic strength.

Determination of Drug Entrapment Efficiency (DEE), Yield and Actual Drug Loading

PNPs and engineered PNPs (M-PNPs and M-PEG-PNPs) were dissolved in 1 mL of acetonitrile followed by addition of 2 mL of methanol to precipitate the polymer. The

sample was centrifuged for 5 minutes at 21,000 X g, and AmB was estimated by high-performance liquid chromatography (HPLC) method described by Echevarria *et al.* (21), with minor modifications, using a C18 column (250×34.6 mm, 5 mm particle size) (Shimadzu, Kyoto, Japan), preceded by a guard column (45×34.6 mm). The mobile phase was comprised of acetonitrile: acetic acid (1%): water (41:43:16 v/v) at a flow-rate of 1.5 mL /min, and the chromatography was carried out at room temperature. The UV detection was performed at 405 nm using SPD-M10Avp diode array UV detector (Shimadzu, Kyoto, Japan). The retention time was found to be 4.3 min. The percent drug entrapment efficiency (%DEE) was calculated by the following Eq. (I):

$$\mathrm{DEE}(\%) = \frac{\text{Mass of drug in engineered PNPs}}{\text{Mass of drug used in formulation}} \times 100 \quad \text{(I)}$$

The purified nanosuspension was ultra-centrifuged (Z 36 HK, Hermle Labortechnik GmbH Wehingen, Germany) at 31,000X g for 1 h at 4±1°C, the supernatant was discarded and pellet was freeze-dried. The yield of various engineered PNPs was calculated using Eq. (II) while actual drug contents of engineered PNPs were calculated using Eq. (III).

$$\text{Nanoparticles yield}(\%\,\mathrm{w/w}) = \frac{\text{Mass of recovered engineered PNPs}}{\text{Total mass of polymer and drug added}} \times 100 \quad \text{(II)}$$

$$\text{Actual drug loading}\,(\%\,\mathrm{w/w}) = \frac{\text{Mass of drug in engineered PNPs}}{\text{Mass of engineered PNPs recoverd}} \times 100 \quad \text{(III)}$$

Transmission Electron Microscopy (TEM)

The shape and size of engineered PNPs were determined in a TEM (H7500, Hitachi Ltd., Tokyo, Japan). The aqueous dispersion was placed over a 400 mesh carbon-coated copper grid followed by negative staining with phosphotungstic acid solution (3% w/v, adjusted to pH 4.7 with KOH) and placed at the accelerating voltage of 95 KV.

Atomic Force Microscopy (AFM)

AFM was performed with a Digital Nanoscope IV Bioscope (Veeco Instruments, Santa Barbara, CA, USA) as described elsewhere (22). The vibration-damped microscope was equipped with pyramidal Si3N4 tips (NCH-W, Veeco Instruments, Santa Barbara, CA, USA) on a cantilever with a length of 125 μm, a resonance frequency of about 220 kHz and a nominal force constant of 36 N/m. All measurements were performed in the tapping mode. The scan speed was proportional to the scan size with a scan frequency from 0.5 to 1.5 Hz. Images were obtained by displaying amplitude, height and phase signal of the cantilever in the trace direction recorded simultaneously.

Lectin Binding Assay

In vitro ligand-specific activity was performed to assess the surface orientation and availability of mannose ligand after formation of engineered PNPs using Concanavalin A (Con A) lectin following reported method with slight modifications (23). Briefly, 200μL (1% w/v) of M-PNPs and M-PEG-PNPs were taken separately and diluted 10 times with PBS (pH 7.4), 1 mL of Con A (varying concentrations of Con A; 25–200 μg/L) in PBS (pH 7.4) with 5 mM of calcium chloride and 5 mM of magnesium chloride was added, and time-dependent increase in turbidity at 550 nm was monitored spectrophotometrically (Shimadzu 1601 UV/VIS spectrophotometer, Japan) for 1 h.

In Vitro Release Study

In vitro release was studied by dialysis method and quantified by HPLC. Briefly, 10 mg AmB equivalent of various formulations of engineered PNPs were suspended in 2 mL of phosphate buffer saline (PBS, pH 7.4) containing 5% v/v of DMSO in a dialysis bag (MWCO 5 KDa, AnaSpec, Inc., San Jose, CA, USA**)** and dialyzed against 50 mL of PBS: DMSO (95:5% v/v) at a speed of 50 rpm. Samples (500 μL) were collected at known intervals and replenished by PBS: DMSO (95:5 % v/v) while maintaining strict sink condition throughout the experiment (1). To simulate PNP release in the endosomal compartment of macrophages, release rate was also determined in sodium acetate buffer (pH 5.5; 0.2 M).

Flow Cytometric Analysis

J774A.1 macrophages cell line was maintained as an adherent culture in humidified atmosphere (5% CO_2) at 37± 1°C in Dulbecco's Modified Eagle Medium (DMEM) (4.5 g/L glucose) with glutamax-I (Gibco, BRL, Gaithersburg, MD, USA) supplemented with 10% heat-inactivated Foetal Calf Serum (FCS), 100 IU/mL penicillin and 100 IU/mL streptomycin. For experiments, cells were detached mechanically and adjusted to the required concentration of viable cells by counting in a haemocytometer.

J774A.1 macrophages were incubated with RITC-labeled, engineered NPs formulations and analyzed at different time intervals. At the end of each interval the cells were harvested, excess of formulations were removed by washing with ice-cold PBS containing 0.01% sodium azide and 5% FCS, and finally resuspended in fluorescent assisted cell sorting (FACS) buffer (BD Biosciences, CA, USA). Phagocytosis was measured in a flow cytometer (BD FACS Calibur, CA, USA) equipped with an argon ion laser exciting at a wave length of 488 nm. For each sample, 10,000 events were collected. Cell-associated RITC was measured by Cell Quest Software (BD-IS, NJ, USA) (24,25).

Ex Vivo Antilieshmanial Activity

Macrophages J774A.1 (10^5 cells/well) were infected with promastigotes (*L. donovani,* Dd8) at multiplicity of infection of 10:1 (parasites/macrophages) in 16-well chamber slides (Nunc, IL, USA) and incubated at 37±1°C in 5% CO_2 for 12 h. Different concentrations of plain as well as engineered

PNPs formulations in RPMI-1640 medium were added to wells in triplicate and examined for intracellular amastigotes after washing followed by methanol fixing and finally Giemsa staining of the slides. At least 100 macrophage nuclei were counted per well for calculating percentage infected macrophages and number of amastigotes per 100 macrophages. The untreated infected macrophages were used as control. Percent parasite inhibition in treated wells was calculated using the following formula (26,27):

$$\% \text{ Parasite inhibition} = 100 - \frac{T}{C} \times 100$$

where T and C are the number of parasites in treated as well as control samples per 100 macrophages nuclei, respectively.

In Vivo Biodisposition Study

In vivo biodisposition study was conducted following the protocol approved by the Institutional Animals Ethical Committee of Dr. H. S. Gour University, Sagar, India. Proper humane care of animals was taken during study period. In order to establish the *in vivo* targeting potential of proposed carrier in macrophage-rich organs (liver, kidney, spleen, lung and lymph node), biodisposition study was performed on adult male Swiss albino mice weighing 30–35 g and data compared with plain drug solution. Animals were divided into four groups, each comprised of 24 animals (3 animals per time-point, and a control group). The AmB solution, PNPs and engineered PNPs formulations (M-PNPs, M-PEG-PNPs) were injected i.v. into tail vein, the animals were sacrificed at specified time interval and organs were weighed, processed and analyzed by HPLC (21).

Statistical Analysis

Statistical analysis was performed with Graph Pad Instat Software (Version 3.00, Graph Pad Software, San Diego, California, USA) by one-way ANOVA followed by Tukey–Kramer test for multiple comparisons. Difference with $p<0.05$ was considered statistically significant.

RESULTS

The novel conjugates of PLGA viz. M-PLGA (without spacer) and M-PEG-PLGA (with PEG spacer) were synthesized (Fig. 1 A, B) and characterized by FTIR (Fig. 2 A, B). The FTIR results confirmed the synthesis of these novel conjugates.

PNPs, M-PNPs and M-PEG-PNPs were prepared by emulsion solvent evaporation method with slight modifications using sodium cholate as surfactant (20,28), which was very effective in reducing the size while a very low amount remained associated with PNPs surface (28). The unloaded and AmB-loaded PNPs were characterized for particle size, shape and surface charge using various techniques.

The size of blank PNPs, M-PNPs and M-PEG-PNPs was found to be 146±26, 157±12.2 and 178±10.4 nm, respectively. Size of PNPs was not increased considerably after AmB loading possibly due to encapsulation of monomeric form of AmB during PNPs formation (Table I). The PDI data suggested that PNPs formed were monodispersed; M-PNPs and M-PEG-PNPs depicted a marginal increase in PDI as compared to PNPs owing to the hetrogenecity of polymer mixture used for preparation.

The % DEE of PNPs was observed to be 53.0±1.5%, while its engineered version showed higher % DEE corresponding to 69.4±2.4 for M-PNPs and 81.2±2.1 for M-PEG-PNPs. The drug loading of various PNPs, M-PNPs and M-PEG-PNPs was found to be 2.81±0.16, 4.2±0.26 and 5.9±0.46 %, respectively (Table I).

The zeta potential of PNPs, M-PNPs and M-PEG-PNPs was found to be -43.04±1.4, −26.9±1.4, −34.9±1.9 mV, respectively. The zeta potential of AmB-loaded PNPs, M-PNPs and M-PEG-PNPs was found to be −46.2±1.2, −28.5±1.5, −37.2±1.1 mV, respectively, suggesting insignificant change ($P>0.05$) in comparison to unloaded PNPs (Table I).

TEM was used to investigate the size and shape of engineered PNPs. TEM photographs suggested that all M-PNPs and M-PEG-PNPs were spherical in shape and in nanometric range (Fig. 3 A, B). However, the surface of engineered PNPs was relatively less spherical and smooth in comparison to PNPs. M-PEG-PNPs showed greater size variation as compared to M-PNPs.

Size and morphology of engineered PNPs were studied by AFM to provide additional evidences regarding their spherical geometry. Further, the surface morphology of these engineered PNPs was found to be smooth with slight aggregation (Fig. 4 A, B).

Fig. 5(A, B) depicts turbidity (absorbance) changes after addition of varying concentrations of lectin to M-PNPs and M-PEG-PNPs formulations. It is clearly evident by high absorbance that mannose in M-PEG-PNPs is capable of interacting with the lectin receptors to a higher extent than M-PNPs (Fig. 5 A, B). The rate of agglutination depends on lectin concentration. The extent of aggregation increased as lectin concentration was increased from 25 to 200 μg/mL,

Table I. Characterization of Plain and Engineered PNPs

Formulations		Size (nm) [a] (PDI) [a]	DEE [a] (% *w/w*)	Actual drug loading [a] (% *w/w*)	Nanoparticles yield [a] (% *w/w*)	Zeta potential [a] (mV)
PNP	Blank	146±26 (0.081±0.031)	–	–	84.0±1.20	−43.04±1.4
	AmB loaded	154±16.3 (0.112±0.015)	53.0±1.5	2.81±0.16	68.50±3.4	−46.2±1.2
M-PNPs	Blank	157±12.2 (0.155±0.021)	–		76.5±2.5	−26.9±1.4
	AmB loaded	164±9.9 (0.142±0.015)	69.4±2.4	4.2±0.26	68.7±1.9	−28.5±1.5
M-PEG-PNPs	Blank	178±10.4 (0.132±0.015)	–		70.8±1.4	−34.9±1.9
	AmB loaded	198±13.4 (0.162±0.015)	81.2±2.1	5.9±0.46	64.7±1.2	−37.2±1.1

[a] Errors presented as standard deviation; $n=3$

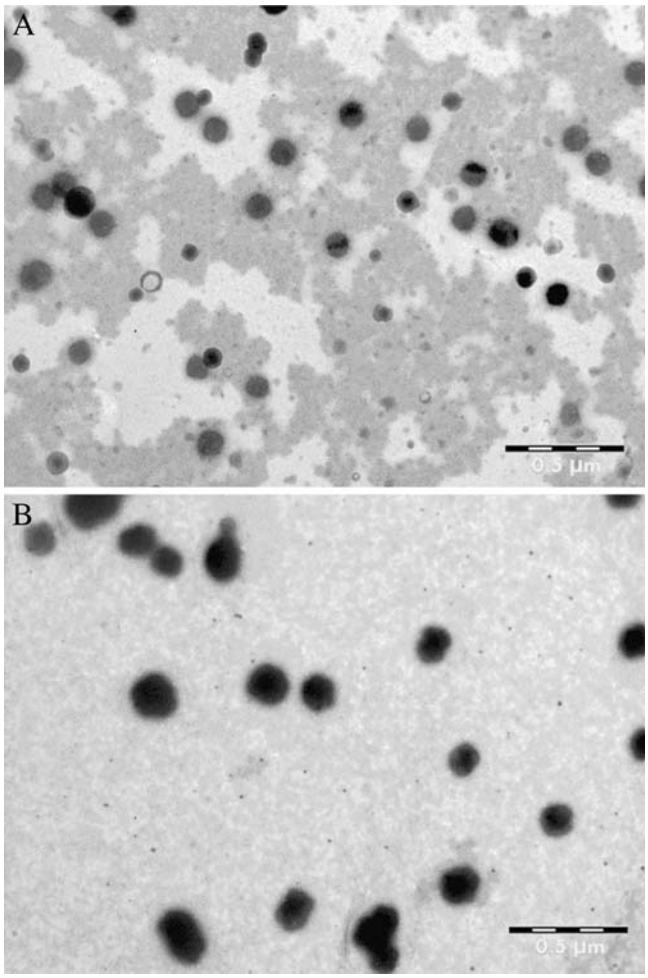

Fig. 3. TEM photomicrographs of engineered PNPs at 80000 magnifications; (**A**) M-PNPs, (**B**) M-PEG-PNPs. *Bars* represent 0.5 µm.

while time was increased from 5 to 45 min (Fig. 5 A, B). The saturation of binding sites may be responsible for insignificant increase in absorbance beyond 200 µg/mL Con A concentration. After 45 min no change in absorbance was observed. These results are in agreement with our previous findings (29).

When conducting *in vitro* drug release study from the formulation containing lipophilic drug, sink condition must be maintained during the release study. Because AmB is a highly lipophilic drug, the sink condition during the release study was maintained by addition of 5% v/v of DMSO in the phosphate buffer. It was observed that at physiological pH, the drug release from the PNPs, M-PNPs and M-PEG-PNPs followed characteristic sustained pattern. The AmB released over 216 h from formulations PNPs, M-PNPs and M-PEG-PNPs was 90.1±1.1%, and 91.3±1.5%, 93.5±1.5%, respectively (Fig. 6A). Release rate was also determined in sodium acetate buffer (pH 5.5; 0.2 M) to simulate PNPs release in endosomal compartment of macrophages. The AmB released in 216 h from the PNPs, M-PNPs and M-PEG-PNPs was 91.7 ±1.79%, 92.8±1.34%, 94.59±1.07%, respectively at pH 5.5, suggesting faster drug release from PNPs at endosomal pH (lower pH) (Fig. 6B).

Flow cytometry study suggests a sharp increase in fluorescence up to 6 h (26.34±1.21%) for PNPs and 4 h for M-PNPs (44.60±1.32%) and M-PEG-PNPs (67.51±1.25%). The results suggested that uptake did not increase considerably on further increasing the time. The percentage uptake at various time intervals from these formulations is presented in Fig. 7.

The effect of various concentrations of free and encapsulated AmB was evaluated against *L. donovani*-infected macrophage amastigote model. The activity of AmB (1 µM) as plain drug, AmBisome®, and PNPs, M-PNPs, M-PEG-PNPs showed percent inhibition of 61.77±2.34, 83.43±2.04, 74.5±1.45, 80.19±2.76 and 87.5±3.10, respectively (Table II). The results suggest increased activity of engineered PNPs in macrophage amastigote model that could account for more efficient uptake of particles by infected macrophages in comparison with free drug.

The amount of AmB present in liver, kidney, spleen, lung and lymph node at different time intervals after i.v. administration of free AmB revealed that maximum accumulation of the drug in these organs was achieved after 0.5 h. Maximum amount of drug accumulated after 0.5 h following i.v. administration of free AmB was 0.62±0.031 µg/g in liver, 0.28±0.01 µg/g in spleen, 0.28±0.014 µg/g in kidney, and 0.08±0.004 µg/g in lung, which declined constantly up to 72 h (Fig. 8 A–E). However, the maximum amount of drug accumulated in lymph node, liver, lung, kidney and spleen is considerably less with free drug in comparison to engineered PNPs. Entrapment of AmB into the engineered PNPs leads to its increased accumulation in liver, spleen, lung and lymph node significantly. Uptake was increased (about 2–10 times) as compared to plain drug solution following the i.v. administration of formulation (Fig. 8 A–E).

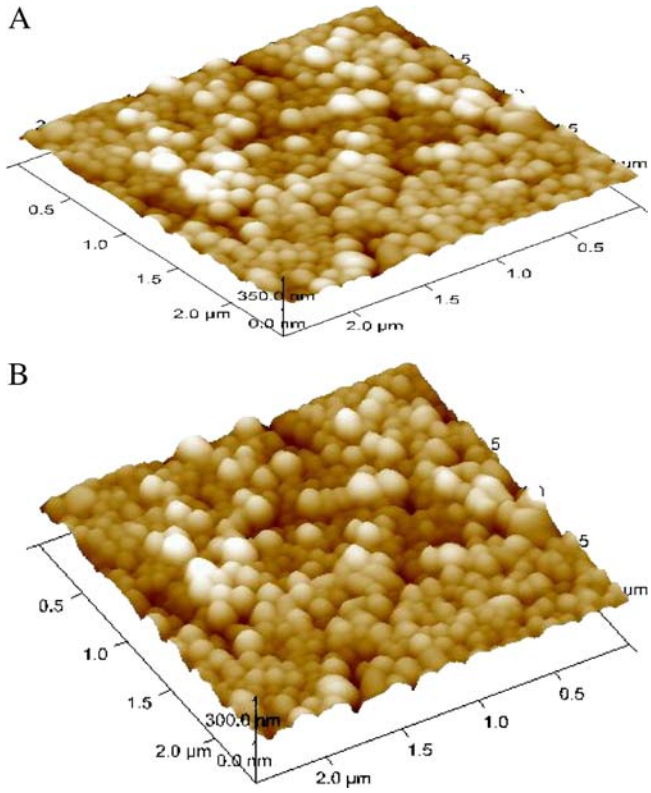

Fig. 4. AFM Photomicrographs of engineered PNPs at tapping mode; (**A**) M-PNPs, (**B**) M-PEG-PNPs.

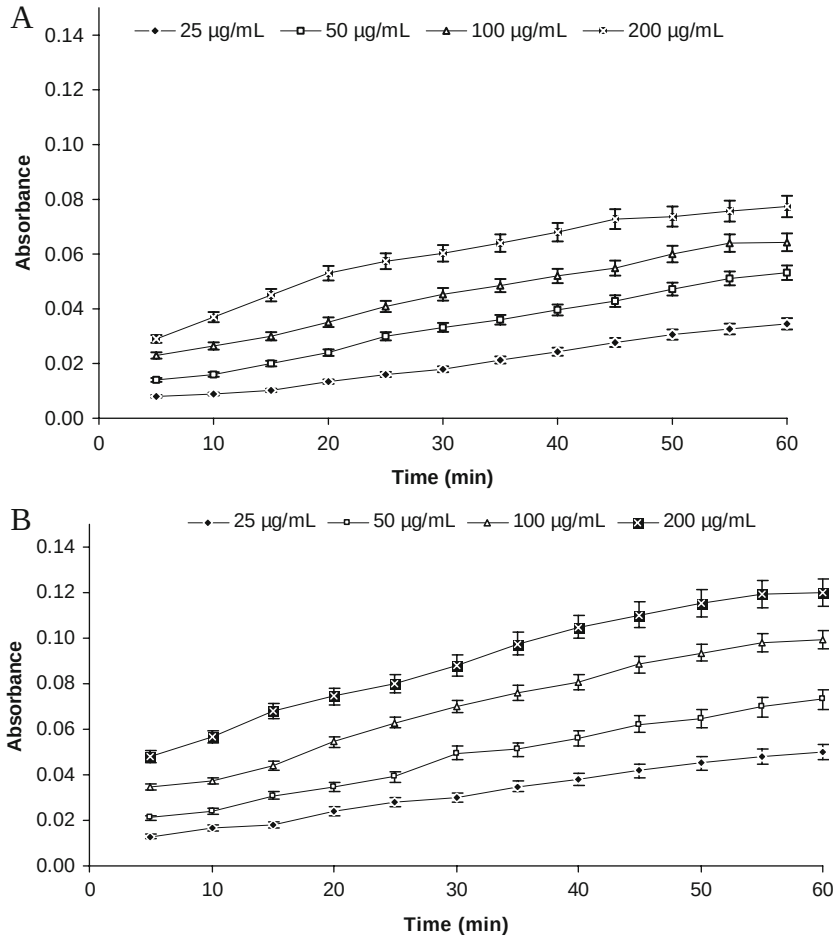

Fig. 5. *In vitro* ligand agglutination of engineered PNPs at various Con A concentrations; (**A**) mPNPs, (**B**) m-PNPs. Absorbance was measured at 550 nm. Values represent mean ± SD (n=3).Absorbance was measured at 550 nm. *Bars* represent mean ± SD (n=3).

DISCUSSION

The NPs were engineered by synthesizing various conjugates of PLGA with mannose either directly or via spacer, followed by preparation of NPs from these conjugates. RITC-PLGA conjugate was also prepared for formulation of RITC labeled carrier for *in vitro* cell uptake study.

The various physicochemical properties of AmB, like limited solubility in water, oil and organic solvents, along with aggregatory nature, are the major concerns for low content of AmB, as reported earlier (20). Therefore, efforts were made to enhance the AmB loading by employing the principle of cosolvency and lowering the pH. The objective was to select an organic phase, which was able to solubilize both AmB and the PLGA. Moreover, it has been reported that solubility of AmB in different solvents can be increased by acidification (30). AmB is insoluble in most of the solvents, necessitating the use of DMSO as co-solvent. The addition of a polar solvent like DMSO to the dispersed organic phase decreases mean size of PNPs and narrows down their size distribution (20,30). Therefore, in the present investigation, a cosolvent, and acidic pH of medium were used to maximize AmB loading. DMSO: DCM ratio and pH of organic phase were optimized to obtain small PNPs and narrow size distribution with good sphericity. DMSO: DCM mixture (25:75 v/v) and pH 3.0 yielded nanometric PNPs with small PDI and acceptable drug content. The probable reason for such small particle size (154±16.3) and low PDI(0.112±0.015) may be ascribed to low density (1.10 g/cm3) and higher miscibility of DMSO in water, as DCM has a high density of 1.32 g/cm3, which alone does not favor a good dispersion. Further, addition of DMSO resulted in more stable and more viscous emulsion droplets as solvent extraction is faster during the evaporation of DCM under vacuum. The droplet fusion that was prevented also favored a narrower size distribution and a lower mean diameter (20). Further, probable reason of high AmB content could be high solubility of AmB in acidic pH that caused higher association with PNPs (30).

The drug content in the PNPs is affected by the drug–polymer interaction and drug miscibility in the polymer. The hydrophobic core of PLGA facilitates the loading of amphiphilic AmB. Polymer gets precipitated slowly because of the slow rate of solvent removal, allowing more time for drug molecules to partition into the aqueous phase, thus resulting in low % DEE. However, increased entrapment efficiency was observed in the case of the engineered version of PNPs (M-PNPs and M-PEG-PNPs). The probable reason for such

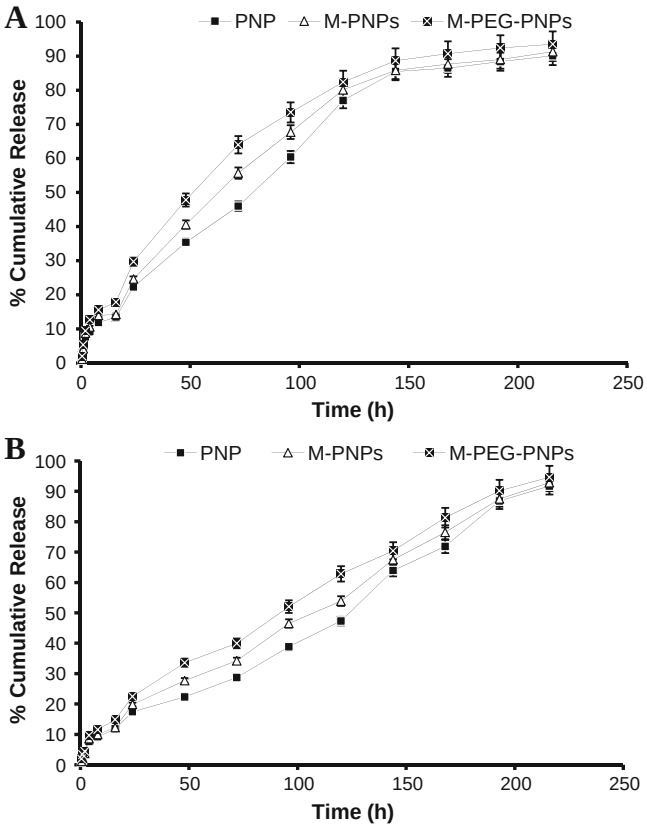

Fig. 6. *In vitro* AmB release from engineered PNP at 37±0.5°C; (**A**) PBS (pH 7.4, 5% v/v DMSO), (**B**) sodium acetate buffer (pH 5.5, 5% v/v DMSO). *Bars* represent mean ± SD (n=3).

increase might be higher drug–polymer miscibility leading to greater drug incorporation as reported earlier for Dexamethasone or Flutamide-loaded PLGA/PLA nanoparticles (31). The significant rise in drug content in M-PNPs and M-PEG-PNPs might be due to an increase in drug–polymer interaction (between hydroxyl group of mannose and PEG and amine group of AmB) and miscibility for amphiphilic AmB. Budhian *et al.* (32) also suggested that acidic end-group of PLAG is responsible for drug incorporation, and increase in chain length may increase the drug-polymer interactions leading to improved the drug incorporation efficiency (Table I).

Measurement of zeta potential allows predictions about the storage stability of colloidal dispersion. In general, particle aggregation is less likely to occur for charged particles (high zeta potential) due to electrical repulsion. Zeta potential of NPs was negative due to the presence of terminal carboxylic groups in the polymers. The reduction in zeta potential after mannosylation was possibly due to the masking of free carboxylic group utilized for conjugation. High absolute value of zeta potential indicates higher electric charge on the surface of the drug-loaded NPs, which causes strong repulsion among the particles and hence prevents aggregation in buffered solution.

Low molecular weight PNPs are reported to exhibit zero-order release profiles, particularly with lipophilic drug molecules. It is possible that because of the low molecular weight, degradation is playing a dominating role and hence controlling the release rate, thereby exhibiting zero-order release (28).

FACS analysis depicted better internalization efficacy of engineered PNPs than plain PNPs. The results suggested improved rate and extent of uptake by engineered version of NPs. The percentage uptake in J774A.1 macrophages followed this order: engineered PNPs with spacer > engineered PNPs without spacer > plain PNPs. Such internalization by engineered PNPs could be attributed to RME that may lead to enhanced phagocytosis (12). Additionally, higher uptake of engineered PNPs over PNPs also provides the evidence that RME predominated over normal phagocytosis involved in uptake and internalization of particulate carrier. Furthermore, significantly higher (P<0.05) uptake of M-PEG-PNPs was recorded in comparison with M-PNPs, suggesting that spacer played a critical role in uptake and endocytosis. Higher uptake in PNPs with spacer (M-PEG-PNPs) could be ascribed to the fact that spacer provides flexibility and allows ligand to acquire proper orientation for efficient interaction with receptor (8).

The results of *ex vivo* antileishmanial activity suggest increased activity of plain and engineered PNPs in intra-amastigote macrophage model that could account for more efficient uptake of particles in comparison to free drug (9–11). Higher activity was observed with M-PEG-PNPs followed by M-PNPs and PNPs. The higher activity of engineered carrier with spacer (M-PEG-PNPs) could account for more efficient uptake of carrier in comparison to their other counterparts. This may probably be due to the higher uptake by RME that subsequently leads to higher antileishmanial activity.

The biodisposition data suggested that the engineered NPs exhibit the best targeting potential, specifically mannosylated PNPs with spacer as evidenced by recovery of higher and prolonged concentration of administered dose by macrophage-rich tissues. Engineered PNPs showed significant increase in the uptake by these macrophage-rich organs due to RME (9). The slightly lower uptake was obtained in M-PEG-PNPs to that of M-PNPs for initial 4 h, but as the time increased (up to 72 h) M-PEG-PNPs got accumulated in higher concentration. Thus, engineered PNPs with spacer (M-PEG-PNPs) showed both increased rate as well as extent of

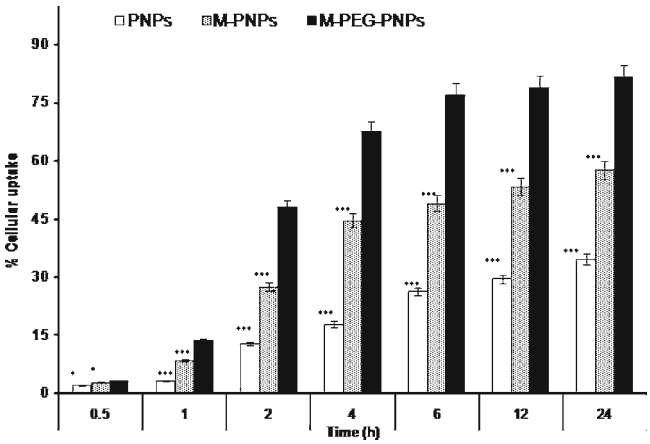

Fig. 7. Uptake of AmB-loaded RITC-labeled plain and engineered PNPs by J774.A1 macrophages. All groups were compared with M-PEG-PNPs, where * indicated significant difference (p<0.05) and *** indicated highly significant difference (p<0.001). *Bars* represent mean ± SD (n=3).

Table II. Antileishmanial Activity of Engineered PNPs Against Amastigotes Macrophage Model

Formulations code	Percent inhibition at AmB concentration (μM)[a]				
	0.05	0.10	0.20	0.50	1.00
AmB solution	21.62±1.16***	31.45±1.08***	49.19±1.21***	52.41±2.78***	61.77±2.34***
AmBisome®	38.45±1.12 ns	58.87±2.09 ns	70.60±1.10 ns	78.46±2.13 ns	83.43±2.04 ns
PNPs	25.10±1.10***	41.20±2.19***	61.20±2.17***	66.70±1.98***	74.50±1.45***
M-PNPs	33.35±1.12***	50.00±2.10***	64.70±1.10***	71.19±1.23***	80.19±2.76***
M-PEG-PNPs	40.80±1.23	61.20±2.17	76.50±1.76	81.60±2.98	87.50±3.10

[a] Errors presented as standard deviation; $n=3$
All groups are compared with M-PEG-PNPs, ns- non significant $p>0.05$;
*significant $p<0.05$;*** very highly significant $p<0.001$

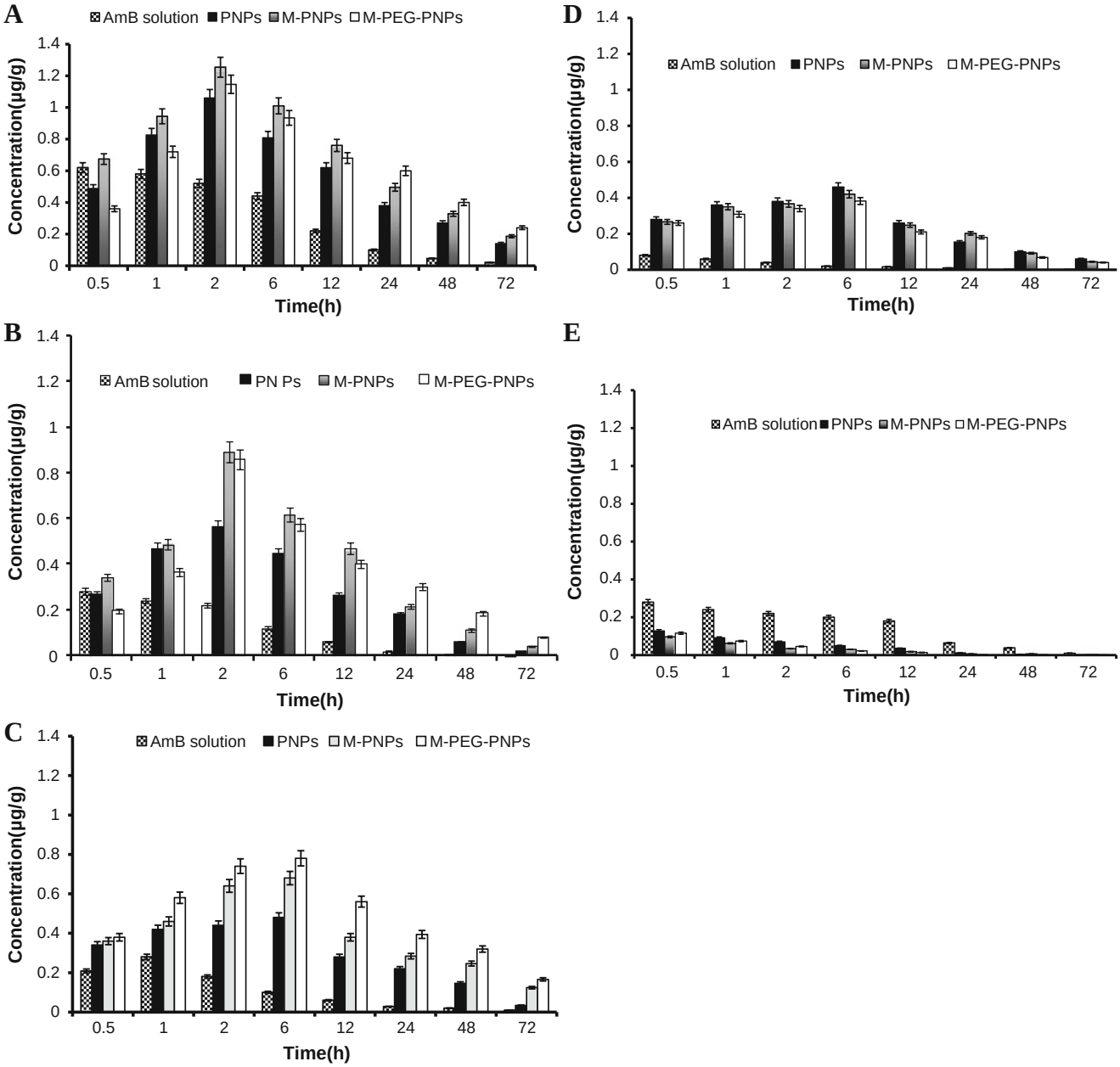

Fig. 8. Biodisposition pattern of engineered PNPs in various organs; (**A**) liver, (**B**) spleen, (**C**) lymph node, (**D**) lungs, (**E**) kidney. *Bars* represent mean ± SD ($n=3$).

uptake, specifically to macrophages, in comparison to plain and engineered counterparts without spacer.

CONCLUSION

We have reported the development of engineered PNPs using polymer-ligand conjugates, which were characterized and evaluated for targeting potential to macrophages. Higher AmB entrapment obtained in engineered PNPs is an important outcome of this work. Further, we could successfully amend the system in terms of size and use of spacer to enhanced macrophage targeting. Conclusively, spacer contributed significantly in increasing extent and rate of uptake of engineered PNPs.

ACKNOWLEDGEMENTS

Manoj Nahar is thankful to the Indian Council of Medical Research (ICMR, New Delhi, India) for providing financial support. All of the authors express their gratitude to AIMS New Delhi, India; Central Drug Research Institute, Lucknow, India; Bhopal Hospital and Memorial Research Center, Bhopal, India; and Inter University Center, Consortium for Scientific Research, Indore, India for various studies.

REFERENCES

1. Nahar M, Mishra D, Dubey V, Jain NK. Development, characterization and toxicity evaluation of amphotericin B-loaded gelatin nanoparticles. Nanomed Nanotech Bio Med. 2008;4:252–61.
2. Matsumura Y, Maeda H. A new concept for macromolecular therapeutics in cancer chemotherapy. Cancer Res. 1986;46:6387–92.
3. Owais M, Gupta CM. Targeted drug delivery to macrophages in parasitic infections. Cur Drug Del. 2005;2(4):311–8.
4. Chellat F, Merhi Y, Moreau A, Yahia LH. Therapeutic potential of nanoparticulate systems for macrophage targeting. Biomaterial. 2005;26:7260–75.
5. Nahar M, Dutta T, Murugesan S, Asthana A, Mishra D, Saraf S, *et al.* Functional polymeric nanoparticles: an efficient and promising tool for active delivery of bioactives. Crit Rev Ther Drug Carrier Syst. 2006;23:259–318.
6. Sharma A, Sharma S, Khuller GK. Lectin-functionalized poly (lactide-co-glycolide) nanoparticles as oral/aerosolized antitubercular drug carriers for treatment of tuberculosis. J Antimicrob Chemother. 2004;54(4):761–6.
7. Kassab R, Parrot-Lopez H, Fessi H, Menaucourt J, Bonaly R, Coulon J. Molecular recognition by kluyveromyces of amphotericin B-loaded, galactose-tagged, poly (lactic acid) microspheres. Bio Org Med Chem. 2002;10:1767–75.
8. Olivier J, Huertas R, Lee HJ, Calon F, Pardrige WM. Synthesis of Pegylated immunonanoparticles. Pharm Res. 2002;19(8):1137–43.
9. Sett R, Sarkar K, Das PK. Macrophage-directed delivery of doxorubicin conjugated to neoglycoprotein using leishmaniasis as the model disease. J Infect Dis. 1993;168(4):994–9.
10. Ahsan F, Rivas IP, Khan MA, Torres SA. Targeting to macrophages: role of physicochemical properties of particulate carriers-liposomes and microspheres-on the phagocytosis by macrophages. J Contr Rel. 2002;79(1–3):29–40.
11. Basu MK, Lala S. Macrophage specific drug delivery in experimental leishmaniasis. Curr Mol Med. 2004;4(6):681–9.
12. Mukhopadhyay A, Basu SK. Intracellular delivery of drugs to macrophages. Adv Biocheml Eng /Biotech. 2003;84:183–209.
13. Chakraborty P, Bhaduri AN, Das PK. Sugar receptor mediated drug delivery to macrophages in the therapy of experimental visceral leishmaniasis. Biochem Biophy Res Comm. 1990;166:404–11.
14. Yamashita C, Sone S, Ogura T, Kiwada H. Potential value of cetylmannoside-modified liposomes as carriers of macrophages activators to human blood monocytes. Japan J Cancer Res. 1991;82:569–75.
15. Muller CD, Schuber F. Neo-mannosylated liposomes: synthesis and interaction with mouse Kupffer cells and resident peritoneal macrophages. Biochem Biophy Acta. 1989;986:97–101.
16. Barratt GM, Nolibe D, Yapo A, Petit JF, Tenu JP. Use of mannosylated liposomes for *in vivo* targeting of a macrophages activator and control of artificial pulmonary metastases. Ann Instit Past Imm. 1987;138:437–43.
17. Garcon N, Gregoriadis G, Taylor M, Summerfield J. Mannose-mediated targeted immunoadjuvant action of liposomes. Immunology. 1988;64:743–9.
18. Akamatsu K, Nisshikawa M, Takakura Y, Hashida M. Synthesis and biodistribution study of liver-specific prostaglandin E1 polymeric conjugate. Int J Pharm. 1977;155:65. 77.
19. Mitchell JP, Roberts DR, Langley J, Koentgen F, Lambert JN. A direct method for the formation of peptide and carbohydrate dendrimers. Bio Org Med Chem Lett. 1999;9:2785–8.
20. Venier-Julienne M, Benoit J. Preparation, purification and morphology of polymeric nanoparticles as drug carriers. Pharm Acta Helv. 1996;71:121–8.
21. Echevarria I, Barturen C, Renedo MJ, Dios-Vieitez MC. High-performance liquid chromatographic determination of amphotericin B in plasma and tissue; application to pharmacokinetic and tissue distribution studies in rats. J Chromat A. 1998;819:171–6.
22. Westedt U, Kalinowski M, Ms Wittmar, Merdan T, Unger F, Fuchs J, *et al.* Poly(vinyl alcohol)-graft-poly(lactide-co-glycolide) nanoparticles for local delivery of paclitaxel for restenosis treatment. J Contr Rel. 2007;119:41–51.
23. Copland MJ, Baird MA, Rades T, McKenzie JL, Becker B, Reck F, *et al.* Liposomal delivery of antigen to human dendritic cells. Vaccine. 2003;21:883–90.
24. Mishra D, Mishra PK, Dubey V, Nahar M, Dabadghao S, Jain NK. Systemic and mucosal immune response induced by transcutaneous immunization using Hepatitis B surface antigen loaded modified liposomes. Eur J Pharm Sci. 2008;33:424–33.
25. Kocbek P, Obermajer N, Cegnar M, Kos J, Kristl J. Targeting cancer cells using PLGA nanoparticles surface modified with monoclonal antibody. J Contr Rel. 2007;120:18–26.
26. Dube A, Singh N, Sundar S, Singh N. Refractoriness to the treatment of sodium stibogluconate in Indian kala-azar field isolates persists in *in vitro* and *in vivo* experimental models. Parasitol Res. 2005;96:216–23.
27. Guru PY, Agarwal AK, Singhal UK, Singhal A, Gupta CM. Drug targeting in Leishmania donovani infections using tuftsin bearing liposomes as drug vehicles. FEBS Lett. 1989;245:204–8.
28. Senthilkumar M, Subramanian G, Ranjitkumar A, Nahar M, Mishra P, Jain NK. PEGylated Poly (Lactide-co-Glycolide) (PLGA) nanoparticulate delivery of Docetaxel: synthesis of diblock copolymers, optimization of preparation variables on formulation characteristics and *in vitro* release studies. J Biomed Nanotech. 2007;1:52–60.
29. Dutta T, Jain NK. Targeting potential and anti-HIV activity of lamivudine loaded mannosylated poly (propyleneimine) dendrimer. Biochem Biophy Acta. 2007;1770:681–6.
30. Espuelas MS, Legrand P, Irache JM, Gamazo C, Orecchioni AM, Devissaguet J-Ph, *et al.* Poly (ε-caprolacton) nanospheres as an alternative way to reduce amphotericin B toxicity. Int J Pharm. 1997;158:19–27.
31. Panyam J, Labhasetwar V. Targeting intracellular targets. Cur Drug Del. 2004;1:235–47.
32. Budhian A, Siegel SJ, Winey KI. Haloperidol-loaded PLGA nanoparticles: Systematic study of particle size and drug content. Int J Pharm. 2007;336:367–75.